Supplementary data

1. Evaluation of TCR-2 surface ozone against CPCB observations

To assess the robustness of interpolated Tropospheric Chemistry Reanalysis version 2 (TCR-2)[104] surface O_3 data used in this study, the data are compared with available ground-based observations from the Central Pollution Control Board (CPCB)[105] monitoring stations over India. This comparison intended to quantify the magnitude and variability of potential biases in the reanalysis, recognising that CPCB stations are mainly urban or semi-urban and therefore reflect local chemical and meteorological influences rather than regional background ozone relevant for crop exposure[106,107]. Accordingly, TCR-2 and CPCB differences are used to constrain uncertainty in ozone exposure estimates.

1.1 Data and Methodology

Surface O_3 observations are obtained from the Continuous Ambient Air Quality Monitoring Sites (CAAQMS) operated by CPCB and State Pollution Control Boards (SPCBs)[105]. Stations with sufficient data during 2018–2021 are retained (**Table S1**). Surface O_3 measurements available at 15-minutes intervals are aggregated to hourly means and the concentrations are converted from $\mu g/m^3$ to ppbv by dividing with 1.96, assuming standard temperature and pressure[108,109]. TCR-2 surface O_3 data, available at 2-hourly resolution, are linearly interpolated to hourly values and regridded to a higher spatial resolution (0.25° × 0.25°). This linear interpolation of TCR-2 data does not affect peak-scale variability, but ensures temporal consistency with the standard Accumulated Ozone above a Threshold of 40 ppbv (AOT40) definition. The regridded O_3 fields are then sampled at CPCB station locations using nearest-neighbour interpolation.

1.2 Results

1.2.1 Daily, monthly and diurnal evolution of TCR-2 and CPCB ozone

Fig. S1 shows the daily time series of surface O_3 from CPCB observations and TCR-2 reanalysis at individual stations during 2018–2020. Across most stations, TCR-2 reproduces the broad temporal variability and seasonal modulation of surface O_3, including recurring pre-monsoon and post-monsoon enhancements. However, TCR-2 systematically overestimates surface O_3 relative to CPCB observations throughout the period, indicating a systematic bias. Despite this offset, the temporal co-variability between CPCB and TCR-2 remains moderate to strong at most stations. Data gaps in CPCB observations are evident at several stations. Although the daily time series highlights the overall temporal consistency and systematic offset between the two, further insights into the nature of bias. Therefore, monthly (**Fig. S2**) and diurnal climatology (**Fig. S3**) are computed to assess whether the overestimation varies with season and time of day, which are more important for the ozone exposure metrics. The monthly climatology of surface O_3 (**Fig. S2**) demonstrates that the positive bias persists across all months, with higher overestimation during pre-monsoon (March–May) and winter (December–February) seasons at most stations. The station-wise mean diurnal cycle of surface O_3 from CPCB and TCR-2 is (**Fig. S3**) also consistent with the daily time-series and TCR-2 systematically overestimates surface O_3 across most stations. Daytime overestimation is stronger at many sites (AP001, KA011, UP008, UP014, DL004), consistent with enhanced photochemical production, whereas nighttime biases at some stations (AP002, DL009, WB013, GJ001) likely reflect differences in nocturnal chemistry, boundary-layer dynamics, or representativeness between point measurements and gridded reanalysis. Despite systematic differences in magnitude, TCR-2 reproduces the observed diurnal and monthly variability at most stations, indicating that the reanalysis captures the large-scale temporal controls on surface O_3 over India.

Station-wise statistical metrics, including mean bias, root mean square error (RMSE), Pearson correlation (R) and the number of valid data points are summerised in **Table S2**. Across the stations, TCR-2 exhibits systematic positive bias, with its magnitude typically ranging from 9 to 37.7 ppbv. Correlations are moderate (R ≈ 0.28–0.65), indicating that temporal variability is reasonably captured despite differences in absolute concentration.

1.2.2 Spatial heterogeneity of surface ozone bias in TCR-2

The magnitude of the TCR-2 − CPCB bias varies substantially across stations (**Fig. S4**), indicating spatially heterogeneous model-observation differences rather than random error. Larger and more spatially coherent positive biases are observed at several stations in northern India (27–37 ppbv in DL004, DL009, DL031, UP008, UP014, HR014, PB001 and WB013), particularly across the Indo-Gangetic Plain (IGP), whereas elevated biases are also evident at individual urban stations in peninsular India (e.g. AP001, AP005, TG003 and KA011). In contrast, several stations in central and southern India exhibit comparatively smaller biases (9–16 ppbv in AP002, MP016, MP003, KL008 and MH016), highlighting the heterogeneous nature of surface ozone discrepancies across regions. All CPCB stations considered are located in urban and peri-urban environments, where surface O_3 concentrations are strongly influenced by local precursor emissions and near-surface chemical processes. In such high-NO_x environments, particularly during winter under VOC-limited regimes, O_3 titration by NO can substantially suppress near-surface O_3 concentrations at these monitoring sites[19]. As a result, point-based CPCB observations may reflect locally reduced O_3 levels that are not representative of the surrounding grid-scale background O_3.

The observed TCR-2 − CPCB values primarily reflect systematic differences in representativeness between urban point-based observations and gridded reanalysis fields. Similar systematic positive biases in modelled surface O_3 relative to CPCB and other surface observations have been widely reported in India in global and regional modelling studies with magnitudes typically ranging from ~1–40 ppbv[110,92,91]. Using simulations from Community Multi-scale Air Quality (CMAQ) and Weather Research and Forecasting (WRF) models, Sharma *et al*[92] showed that modelled daily mean surface O_3 exhibits an overall positive bias (~20.7 ppbv higher than observations), with large spatial heterogeneity and the greatest discrepancies occurring at urban monitoring sites, including Pune and Delhi. They further demonstrated that observed surface O_3 concentrations in highly polluted urban regions are substantially suppressed relative to surrounding areas due to strong NO_x titration, with Delhi exhibiting mean O_3 levels < 25 ppbv compared to 35–60 ppbv in adjacent regions. Similar pattern was noted for other urban centers such as Kolkata and Chennai. These studies further demonstrate that ozone biases vary substantially across regions and urbanisation gradients, reflecting unresolved urban-scale chemistry and transport processes rather than consistent failure of chemical transport models. CMAQ model evaluation study for NO_2 in India by Carambelas *et al*[91] further demonstrate that the magnitude and sign of model − observation biases depend strongly on the observational references used. Using both CPCB surface observations and satellite retrievals, they showed that comparisons against urban CPCB measurements have model high biases in surface NO_2 concentrations, whereas evaluation using satellite-derived tropospheric columns reveals widespread low biases over rural regions of India. Their analysis further suggested that existing emission inventories tend to overestimate emissions in densely populated urban regions, whereas underestimating emissions across rural areas. As a result, reliance on urban surface observations alone is not sufficient for the assessments of model performance or satellite data. These findings reinforce that TCR-2 and CPCB differences primarily reflect

representativeness mismatch and uncertainties in emission spatial allocation rather than systematic deficiencies in reanalysis surface O_3 fields.

Machine-learning (ML) based evaluations further elucidate the regional drivers of surface O_3 bias and provide a strong physical context for the TCR-2 and CPCB differences observed over India[60]. Using surface observations from Tropospheric Ozone Assessment Report (TOAR) network together with TCR-2 chemical reanalysis inputs, Miyazaki *et al*[60] showed that reanalysis products exhibit widespread positive surface O_3 biases over land at low and middle latitudes, with values reaching 20 ppbv in India even during winter months. Their ML framework identified meteorological parameters (surface pressure, temperature and solar radiation) and large-scale chemical drivers [carbon monoxide (CO), VOCs and NO_x reservoir species such as nitric acid (HNO_3) and peroxy-acetyl nitrate (PAN)] as dominant contributors to surface O_3 bias, highlighting the role of unresolved urban-sale chemistry and boundary-layer processes in coarse-resolution reanalyses like TCR-2. The spatial distribution of predicted biases was further shown to correlate with surface characteristics including topography, degree of urbanisation, forest cover and regional precursor emission patterns. Reanalysis ozone biases peak during summer over North America (~30 ppbv) and East Asia (~24 ppbv), regions with dense ground-based monitoring, whereas smaller but persistent biases occur during winter. Across regions, temperature and radiation dominate summer bias, whereas surface pressure and synoptic-scale controls are more influencing during winter. In South Asia, and particularly northern India, the ML analysis revealed a distinct combination of drivers, with NO_x and temperature dominating ozone bias during October–March, reflecting precursor-rich and VOC-limited regimes that enhance urban ozone titration, whereas NO_x reservoir species (HNO_3 and PAN) together with temperature, radiation and CO emissions dominate from spring (March–May) through autumn (October–November). Notably, the ML framework indicated that direct NO_x emissions exert only a limited influence on surface O_3 bias, whereas long-lived reservoir species and VOCs such as ethane (C_2H_6) play a substantially larger role, with particularly strong impacts over northern India. Additional contributions from ammonia (NH_3) were identified over agriculturally intensive regions of northern an eastern India. These findings indicate that the large and seasonally varying positive differences in TCR-2 and CPCB ozone in India, particularly across IGP, primarily arise from unresolved local emission and chemical processes in urban areas, strong precursor loading, and meteorological controls inherent to coarse-resolution reanalyses. The consistency of both bias magnitude and dominant drivers with those identified over observation-rich regions such as North America and East Asia further supports this interpretation. The ML analysis also noted increased uncertainty over polluted regions over South Asia, reinforcing that surface O_3 biases over India primarily reflect scale and process mismatches rather than deficiencies in individual datasets.

A recent comprehensive, nationwide assessment of the CAAQMS operated by the CPCB and SPCBs in India identified substantial data-quality issues for NO_x, including repeated values persisting for extended periods, recurring outliers and unit inconsistencies[111]. The analysis demonstrated that these problems are particularly severe for NO_x, with correction of unit inconsistencies leading to increases in annual mean NO_2 concentrations exceeding 80% at affected sites, substantially altering NO_2-related exposure and health metrics. These unit inconsistencies in NO_2 were identified using internal consistency checks between NO, NO_2 and NO_x (NO_x = NO + NO_2), which allow scaling and reporting errors to be diagnosed directly from the observations. Earlier work further showed that NO and NO_2 were intermittently reported in ppb rather than $\mu g/m^3$ at several sites in Delhi and Kanpur, and in some

cases switched between units at different times of the year, leading to large errors in reported concentrations[112]. In contrast, surface O_3 concentrations were comparatively less affected by data-cleaning procedures, with removal of repeated values and outliers (1–3% on an average across 2019–2023) leading to only marginal changes in long-term, multi-year mean surface O_3[111]. However, as noted by Vohra *et al*[111], unit inconsistency issues can only be diagnosed for pollutants with auxiliary measurements (e.g. NO, NO_2 and NO_x), and therefore cannot be independently identified for O_3 or other species if they exist. CPCB hourly surface O_3 data are therefore used here as an urban observational reference to diagnose systematic differences in TCR-2 surface O_3, rather than as a benchmark for validation or bias correction. Collectively, these factors explain the systematic but non-uniform nature of the differences between TCR-2 and CPCB found here and justify treating the observed bias as a source of uncertainty in ozone exposure and yield-loss estimates.

Table S1. Details of the Central Pollution Control Board (CPCB) monitoring stations selected for evaluation of Tropospheric Chemistry Reanalysis version 2 (TCR-2) surface ozone data in India.

Sl. no	Station Id	Station Name	State	Latitude	Longitude
1	AP001	Secretariat, Amaravati - APPCB	Andhra Pradesh	16.51	80.51
2	AP002	Anand Kala Kshetram, Rajamahendravaram - APPCB	Andhra Pradesh	16.99	81.74
3	AP005	GVM Corporation, Visakhapatnam - APPCB	Andhra Pradesh	17.72	83.3
4	DL004	Aya Nagar, Delhi - IMD	Delhi	28.47	77.11
5	DL009	Dr. Karni Singh Shooting Range, Delhi - DPCC	Delhi	28.49	77.26
6	DL031	R K Puram, Delhi - DPCC	Delhi	28.56	77.19
7	GJ001	Maninagar, Ahmedabad - GPCB	Gujarat	23	72.59
8	HR014	Vikas Sadan, Gurugram - HSPCB	Haryana	28.45	77.02
9	KA011	Silk Board, Bengaluru - KSPCB	Karnataka	12.91	77.62
10	KL008	Plammoodu, Thiruvananthapuram - Kerala PCB	Kerala	8.51	76.94
11	MH016	Gangapur Road, Nashik - MPCB	Maharashtra	20.01	73.78
12	MP003	Bhopal Chauraha, Dewas - MPPCB	Madhya Pradesh	22.97	76.06
13	MP016	Mahakaleshwar Temple, Ujjain - MPPCB	Madhya Pradesh	23.18	75.77
14	PB001	Golden Temple, Amritsar - PPCB	Punjab	31.62	74.87
15	RJ004	Adarsh Nagar, Jaipur - RSPCB	Rajasthan	26.9	75.86
16	TG003	ICRISAT Patancheru, Hyderabad - TSPCB	Telangana	17.52	78.28
17	TN001	Alandur Bus Depot, Chennai - CPCB	Tamil Nadu	12.9	80.1
18	TN004	Velachery Res. Area, Chennai - CPCB	Tamil Nadu	13.01	80.24
19	UP008	Nehru Nagar, Kanpur - UPPCB	Uttar Pradesh	26.47	80.32
20	UP014	Lalbagh, Lucknow - CPCB	Uttar Pradesh	26.85	80.94
21	WB013	Victoria, Kolkata - WBPCB	West Bengal	22.54	88.34

Table S2. Station-wise bias, root mean square error (RMSE), Pearson correlation (R) and data availability for TCR-2 surface ozone relative to CPCB observations (2018–2021). Station names are provided in Table S1

Sl.no	Station Id	Bias (ppbv)	RMSE (ppbv)	Pearson Correlation (R)	Number of data points
1	AP001	22.53	25.64	0.50	11407
2	AP002	14.66	18.81	0.65	12550
3	AP005	28.01	31.97	0.50	11719
4	DL004	32.40	35.26	0.54	12704
5	DL009	27.81	35.77	0.47	12170
6	DL031	31.74	36.51	0.52	12416
7	GJ001	22.27	29.62	0.41	10991
8	HR014	30.77	35.48	0.51	8665
9	KA011	18.56	23.16	0.41	9892
10	KL008	13.34	16.38	0.56	12599
11	MH016	16.27	23.54	0.58	12014
12	MP003	16.34	24.09	0.43	12953
13	MP016	9.11	19.74	0.53	12824
14	PB001	37.77	40.24	0.39	11140
15	RJ004	23.65	27.76	0.49	12834
16	TG003	28.45	31.29	0.54	12972
17	TN001	24.28	28.11	0.42	10717
18	TN004	22.57	25.62	0.45	12819
19	UP008	30.96	36.02	0.34	12785
20	UP014	33.71	37.03	0.28	11416
21	WB013	23.99	28.85	0.48	11000

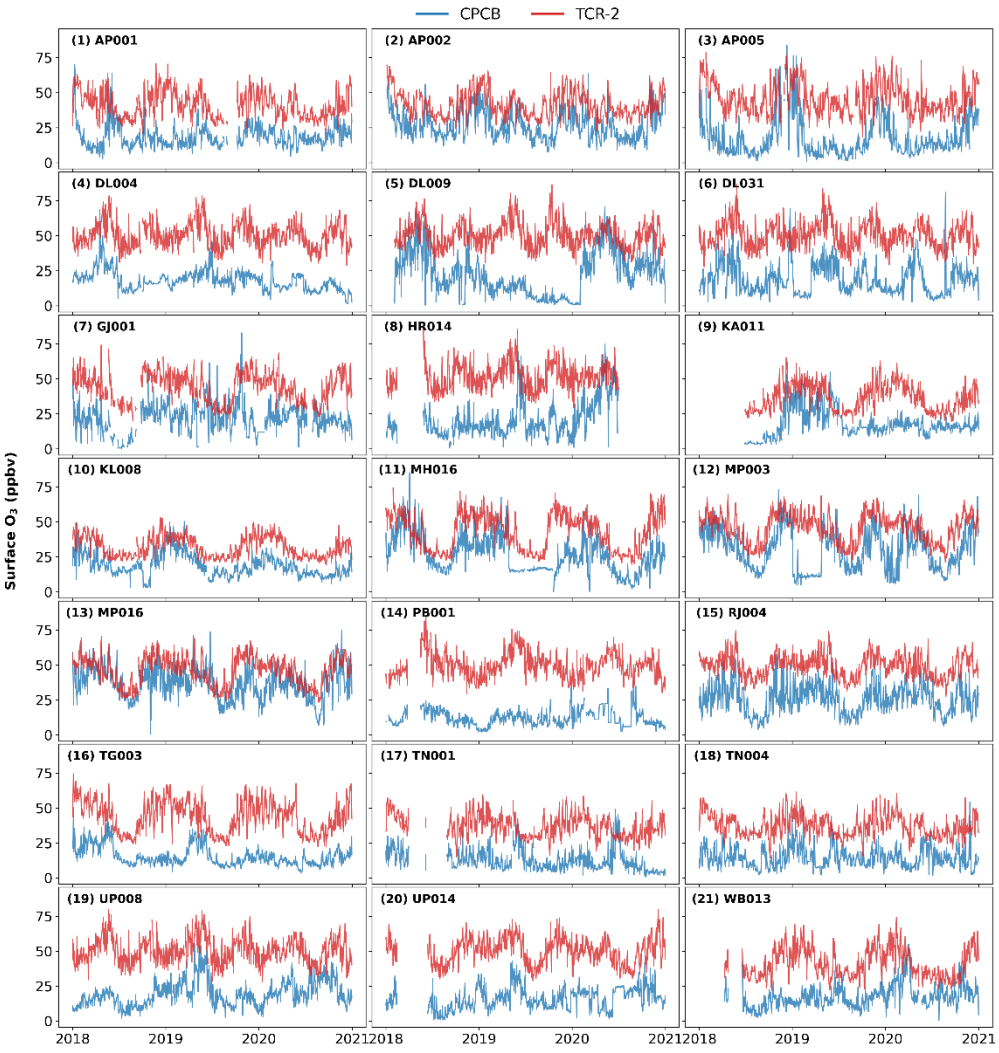

Fig. S1 Station-wise daily time series of surface ozone at CPCB monitoring sites, compared with TCR-2 during 2018–2020. Station names are provided in Table S1.

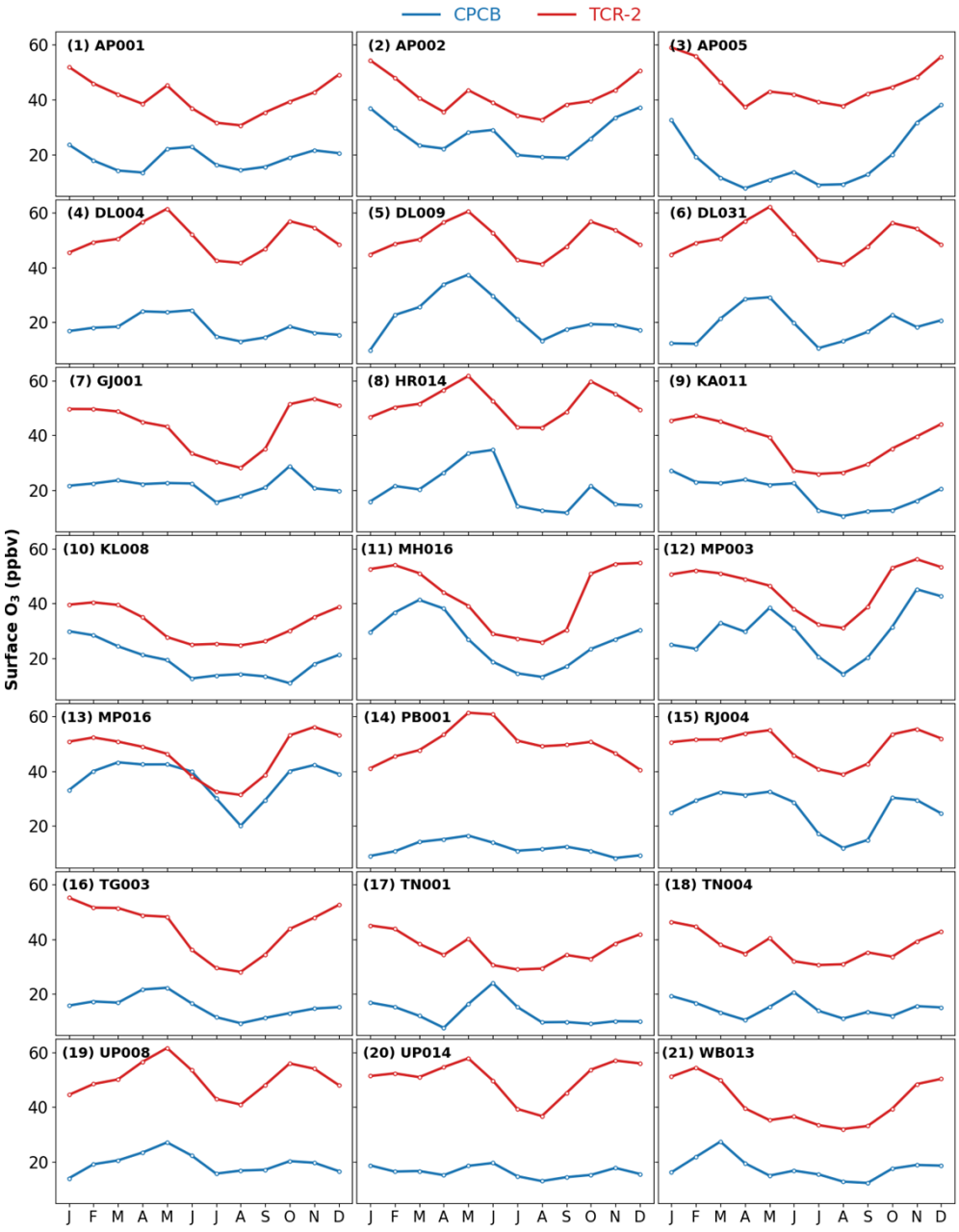

Fig. S2 Station-wise monthly variation of surface ozone at CPCB monitoring sites, compared with TCR-2 during 2018–2020. Station names are provided in Table S1.

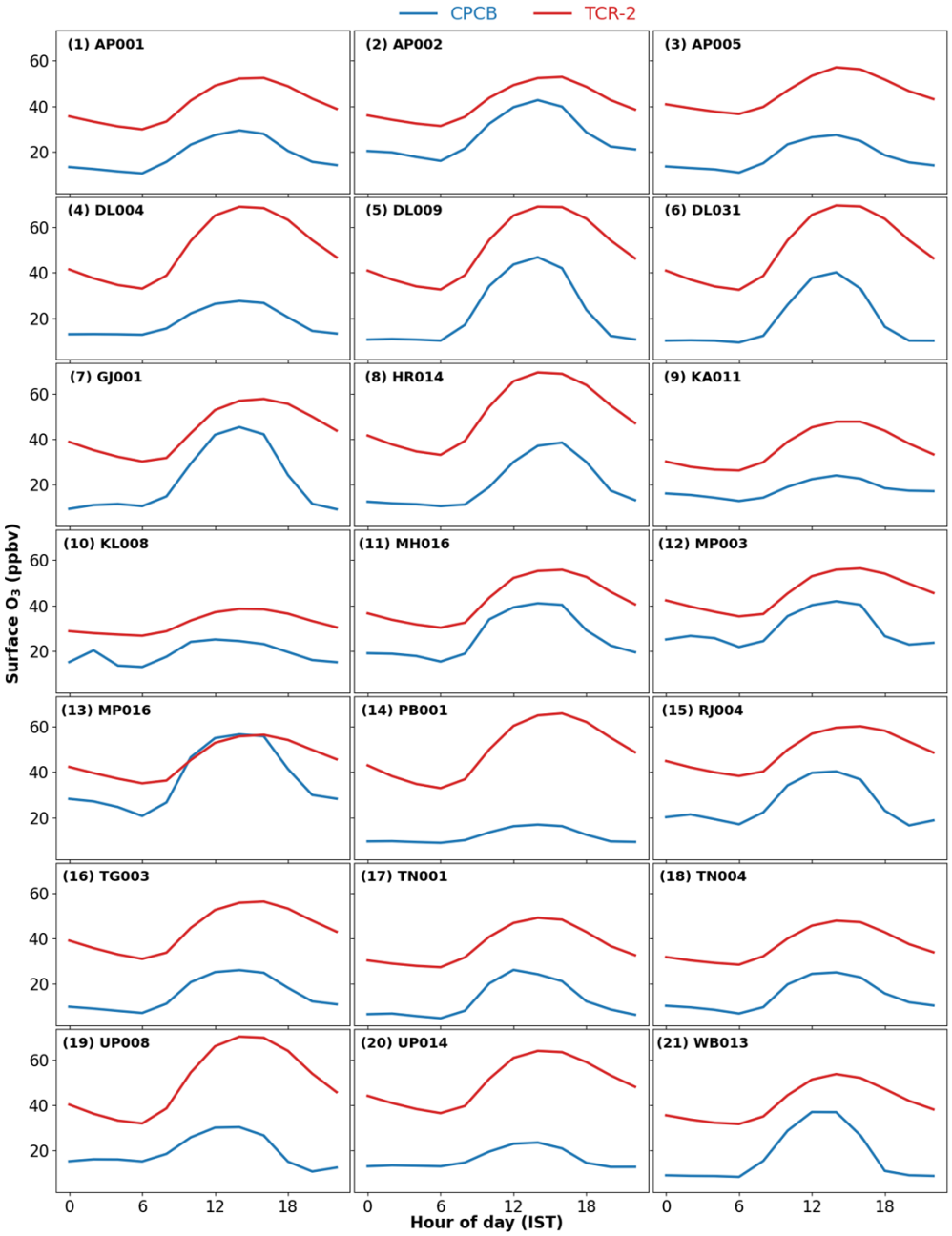

Fig. S3 Station-wise diurnal variation of surface ozone at CPCB monitoring sites, compared with TCR-2 during 2018–2020. Station names are provided in Table S1.

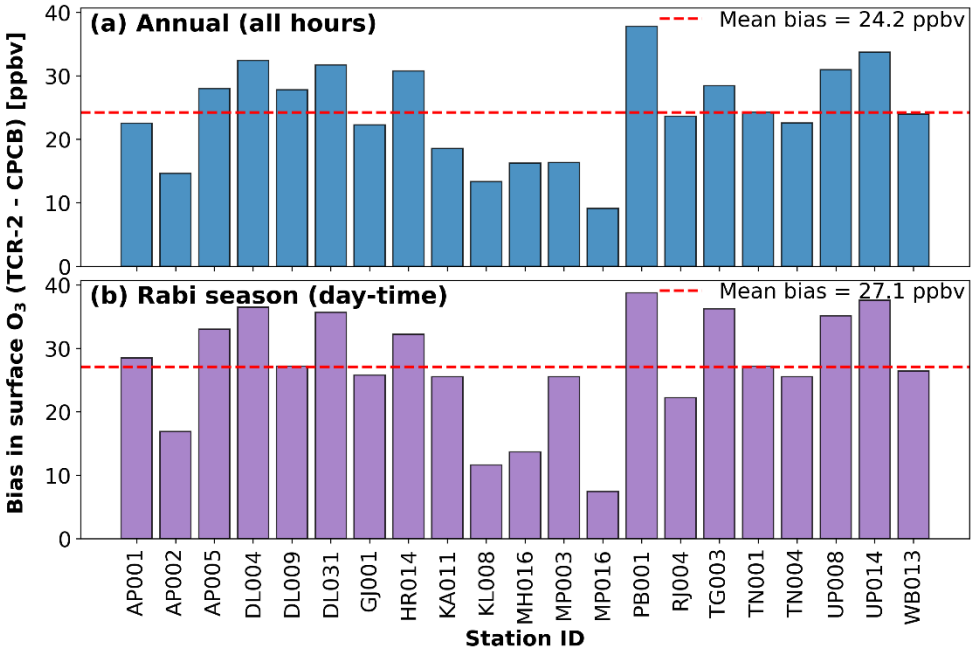

Fig. S4 Mean bias in surface O_3 (TCR-2 – CPCB) across 21 selected CPCB stations for (a) annual average using all hours and (b) rabi season (January–March) daytime average, during 2018–2020. The multi-station mean bias is indicated in the upper right of each panel. Station names are provided in Table S1.

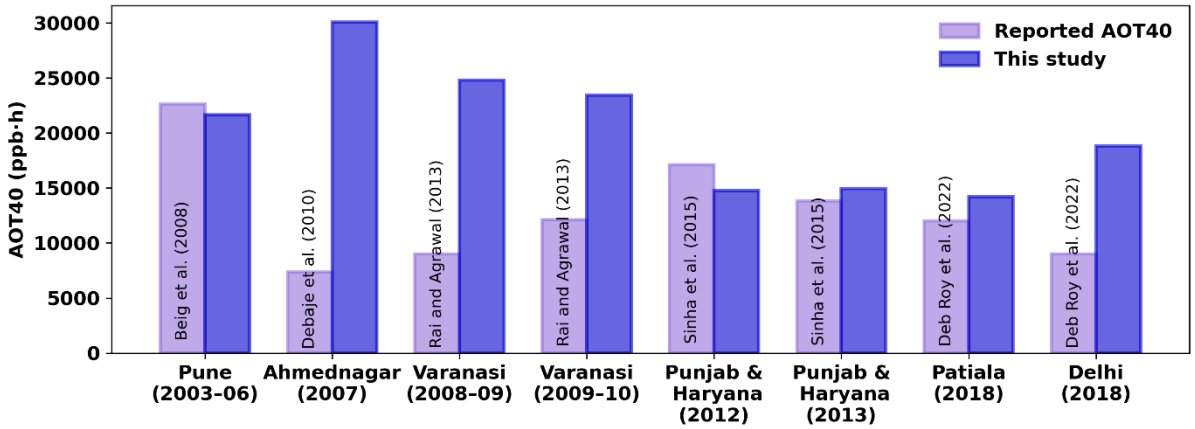

Fig S5 Comparison of AOT40 (ppb.h) values during rabi season in India reported in previous studies and those estimated in this study using TCR-2 surface ozone at the same location, periods and exposure windows. Reported AOT40 values are taken from the literature, and values from this study are computed consistently using TCR-2 data. Site names and study periods are indicated on the x-axis.

2. Implication for food security and trade

Table S3: Top 10 wheat producing countries in the world, their total production of wheat in kilo tonnes (Kt), total import of wheat, total export of wheat, percentage of export to total production, percentage of import to total production and average population (billion people), during 2019–2022. Production, import, export and population data obtained from the statistics of Food and Agriculture Organisation (FAOSTAT)[114].

Sl No	Country	Total Production (Kt)	Total Import (Kt)	Total Export (Kt)	EX/PR (%)	IM/PR (%)	Annual Population (billion)
1	China	542532.10	36268.84	18.77	0.0035	6.69	1.46
2	India	428785.31	3.27	14007.95	3.27	0.001	1.40
3	Russia	340643.91	33.56	114336.00	33.56	0.01	0.15
4	United States of America	192038.08	51.10	98131.98	51.10	0.03	0.34
5	France	141977.93	1030.39	75991.67	53.52	0.73	0.06
6	Canada	124863.89	706.06	89010.68	71.29	0.57	0.04
7	Ukraine	106195.17	33.44	68695.90	64.69	0.03	0.04
8	Pakistan	103269.25	7313.4	301.70	0.29	7.08	0.23
9	Australia	100237.81	972.68	74336.34	74.16	0.97	0.03
10	Germany	89281.2	15224.32	28131.78	31.51	17.05	0.08

Table S4: Export of wheat from India during 2019–2022. Export of wheat in tonnes (t) from India to other countries in the world during 2019–2022. Export data obtained from the statistics of Food and Agriculture Organisation (FAOSTAT). Top 5 importers are highlighted with yellow colour.

Sl No	Country	Export (t)			
		2019	2020	2021	2022
1	Afghanistan		55584.00		37242.01
2	Angola	0.70	13.50	20.50	454.76
3	Australia	2.90	4.85	0.92	0.00
4	Bahrain	365.52	582.81	528.99	342.77
5	Bangladesh	9417.10	378759.70	3668670	2362528.00
6	Barbados				2.00
7	Belgium			1.00	
8	Benin	25.00		1.60	0.60
9	Bhutan	0.24	2310.47	1910.30	2491.00
10	Brunei Darussalam		0.12	0.39	0.53
11	Burundi		2.52		0.40
12	Cambodia		358.00	375.00	75.00
13	Canada	4.31	4.97	17.00	1.33
14	China	62.29	48.59	3690.12	12261.09
15	Congo	2.55	0.60		
16	Cote d'Ivoire	3.10	25.70	4.98	3.65
17	North Korea	1000.00	571.00		
18	Dem. Rep. Congo	1.25	0.95	12.93	0.50
19	Denmark		0.49	1.20	
20	Djibouti			10914.80	92570.59
21	Egypt				61500.00
22	Eq. Guinea		1.84	3.40	4.50
23	Ethiopia			9995.00	2625.00
24	France	960.90	679.4	555.47	0.24
25	Gabon	85.00		51.14	7.50
26	Gambia	3.59	2.75	3.85	0.70
27	Germany		0.40	0.43	0.19
28	Ghana	21.00	60.93	24.94	48.40
29	Guinea	29.61	36.24	42.91	33.00
30	Guinea-Bissau			0.50	
31	Indonesia	4.09		350005.00	939493.00
32	Iran			960.00	
33	Iraq		60.00	417.98	
34	Israel				66950.00
35	Italy		0.30		
36	Japan	12.50	21.58	25.00	6.00
37	Jordan	1182.00	1370.00	3851.35	2453.00
38	Kenya	15.60	98.29	274.53	193.50
39	Kuwait	395.32	383.47	623.73	621.08
40	Lebanon		1.50		1.50

Sl No	Country	Export (t)			
		2019	2020	2021	2022
41	Liberia	0.50	0.11		25.00
42	Madagascar	2.30	11.94	6.75	
43	Malawi	41.46	53.40	33.06	0.25
44	Malaysia	1165.63	5162.86	50220.7	86353.6
45	Maldives	0.45	0.15	0.27	
46	Mauritius	0.06	1.40		
47	Mozambique	1.50	17.64	9.35	42037.60
48	Myanmar		244.00	2343.77	28624.36
49	Nepal	158711.20	296186.50	237845.40	86901.79
50	Netherlands			0.13	0.39
51	New Zealand	27.00	0.27	0.12	
52	Niger	1.50			
53	Nigeria	180.28	216.66	96.53	38514.30
54	Oman	204.81	757.53	76751.15	182544.30
55	Philippines		1426.00	297124.50	251503.10
56	Portugal			0.50	0.20
57	Qatar	28.00	21315.82	125765.00	83396.65
58	South Korea			70000.00	657464.80
59	Rwanda	53.00	34.48	49.12	
60	Saudi Arabia			27.00	915.20
61	Senegal	8.00	8.93	3.82	0.34
62	Seychelles	236.29	205.56	108.40	103.95
63	Sierra Leone	24.85	18.34	1.34	2.00
64	Singapore	33.45	50.97	62.07	3.82
65	Somalia	4260.00	5448.00	6763.99	3193.18
66	South Africa	9.63	23.95	12.76	21.95
67	Sri Lanka	2038.79	72101.65	428073	299531
68	Sudan		0.25	0.80	45000.00
69	Suriname	0.10			
70	Sweden		0.49	0.24	
71	Thailand	0.03	0.20	10614.30	224792.70
72	Togo	2.55	3.74	5.12	
73	Turkey				55515.00
74	Uganda	363.71	718.32	470.28	131.00
75	United Arab Emirates	8796.94	83489.69	476451.20	557197.60
76	United Kingdom	124.61	101.16	85.31	49.08
77	Tanzania	13.35	44.54	71.16	47066.45
78	United States of America	48.35	54.30	78.14	23.93
79	Vietnam	85.06		8015.13	80890
80	Yemen			246532.00	444883.00
81	Zambia	0.05			

Table S5: Export of wheat from India to the Least Developed Countries (LDCs) during 2019–2022. Total Export of wheat in tonnes (t) from India to the LDCs during, total annual population (billion people) and number of severely food insecure people in the LDCs. Export and population data obtained from the statistics of the Food and Agriculture Organisation (FAOSTAT). Data arranged in the decreasing order of export quantity.

Sl No	Country	Continent	Total export (tonnes)	Annual Population (billion)	Severely food insecure people in billion (% of total population)
1	Bangladesh	Asia	6419375.00	0.17	0.018 (10.73%)
2	Nepal	Asia	779644.90	0.029	0.004 (12.93 %)
3	Yemen	Asia	691415.00	0.03	0.004 (11.67%)
4	Djibouti	Africa	103485.40	0.001	0.0002 (16.50%)
5	Afghanistan	Asia	92826.01	0.04	0.009 (23.60%)
6	Tanzania	Africa	47195.50	0.06	0.016(25.50%)
7	Sudan	Africa	45001.05	0.04	0.008(17.43%)
8	Mozambique	Africa	42066.09	0.031	0.013 (40.17 %)
9	Nigeria	Africa	39007.77	0.21	0.041 (19.47%)
10	Myanmar	Asia	31212.13	0.05	0.002 (3.50%)
11	Somalia	Africa	19665.17	0.017	0.007 (42.55%)
12	Ethiopia	Africa	12620.00	0.12	0.022 (19.03%)
13	Bhutan	Asia	6712.01	0.0008	Data not available
14	Uganda	Africa	1683.31	0.04	0.011 (23.83%)
15	Cambodia	Asia	808.00	0.016	0.002 (14.63%)
16	Angola	Africa	489.46	0.03	0.009 (29.50%)
17	Guinea	Africa	141.76	0.013	0.007 (49.37%)
18	Rwanda	Africa	136.60	0.013	Data not available
19	Malawi	Africa	128.17	0.019	0.01 (50.90%)
20	Sierra Leone	Africa	46.53	0.008	0.003 (31.87%)
21	Benin	Africa	27.20	0.01	0.001 (14.30%)
22	Liberia	Africa	25.61	0.005	0.002 (37.37%)
23	Senegal	Africa	21.09	0.016	0.002 (10.77%)
24	Madagascar	Africa	20.99	0.028	0.003 (10.80%)
25	Dem. Rep. Congo	Africa	15.63	0.093	0.037 (39.47%)
26	Togo	Africa	11.41	0.008	0.002 (18.47%)
27	Gambia	Africa	10.89	0.0026	0.001 (26.6%)
28	Burundi	Africa	2.92	0.012	Data not available
29	Guinea-Bissau	Africa	0.50	0.002	0.001 (27.4%)
Total			**8333795.71**	**1.10**	**0.23 (19.78%)**

REFERENCES

19 G. S. Gopikrishnan and J. Kuttippurath, Global tropical and extra-tropical tropospheric ozone trends and radiative forcing deduced from satellite and ozonesonde measurements for the period 2005–2020*, Environ. Pollut*., 2024, **361**, 124869, https://doi.org/10.1016/j.envpol.2024.124869.

60 K. Miyazaki, Y. Marchetti, J. Montgomery, S. Lu and K. Bowman, Identifying drivers of surface ozone bias in global chemical reanalysis with explainable machine learning, Atmos. Chem. Phys., 2025, **25**, 8507–8532, https://doi.org/10.5194/acp-25-8507-2025.

91 A. Karambelas, T. Holloway, G. Kiesewetter and C. Heyes, Constraining the uncertainty in emissions over India with a regional air quality model evaluation, *Atmos. Environ.*, 2018, **174**, 194–203, https://doi.org/10.1016/j.atmosenv.2017.11.052.

92 S. Sharma, S. Chatani, R. Mahtta, A. Goel and A. Kumar, Sensitivity analysis of ground level ozone in India using WRF-CMAQ models, *Atmos. Environ.*, 2016, **131**, 29–40, https://doi.org/10.1016/j.atmosenv.2016.01.036.

104 K. Miyazaki, K. Bowman, T. Sekiya, H. Eskes, F. Boersma, H. Worden, N. Livesey, V. H. Payne, K. Sudo, Y. Kanaya, M. Takigawa and K. Ogoch, Chemical Reanalysis Products, 2019, https://doi.org/10.25966/9QGV-FE81.

105 Central Pollution Control Board (CPCB) (2020). CPCB, Air quality data portal. https://aqinow.org/ccr

106 D. Sharma and D. Mauzerall, Analysis of Air Pollution Data in India between 2015 and 2019, *Aerosol Air Qual. Res.*, 2022, **22**, 210204, https://doi.org/10.4209/aaqr.210204.

107 G. Mills, H. Pleijel, C. S. Malley, B. Sinha, O. R. Cooper, M. G. Schultz, H. S. Neufeld, D. Simpson, K. Sharps, Z. Feng, G. Gerosa, H. Harmens, K. Kobayashi, P. Saxena, E. Paoletti, V. Sinha and X. Xu, Tropospheric Ozone Assessment Report: Present-day tropospheric ozone distribution and trends relevant to vegetation, *Elementa: Sci. Anthropocene*, 2018, **6**, 47, https://doi.org/10.1525/elementa.302.

108 H. Z. Sun, P. Yu, C. Lan, M. W. L. Wan, S. Hickman, J. Murulitharan, H. Shen, L. Yuan, Y. Guo and A. T. Archibald, Cohort-based long-term ozone exposure-associated mortality risks with adjusted metrics: A systematic review and meta-analysis, *The Innovation*, 2022, **3**, 100246, https://doi.org/10.1016/j.xinn.2022.100246.

109 B. J. Finlayson-Pitts and J. N. Pitts, Atmospheric Chemistry of Tropospheric Ozone Formation: Scientific and Regulatory Implications, *Air & Waste*, 1993, **43**, 1091–1100, https://doi.org/10.1080/1073161X.1993.10467187.

110 D. E. Surendran, S. D. Ghude, G. Beig, L. K. Emmons, C. Jena, R. Kumar, G. G. Pfister and D. M. Chate, Air quality simulation over South Asia using Hemispheric Transport of Air Pollution version-2 (HTAP-v2) emission inventory and Model for Ozone and Related chemical Tracers (MOZART-4), *Atmos. Environ.*, 2015, **122**, 357–372, https://doi.org/10.1016/j.atmosenv.2015.08.023.

111 K. Vohra, M. S., A. Chakraborty, H. Shah, B. As. and J. Pakki, Urgent issues regarding real-time air quality monitoring data in India: Unveiling solutions and implications for policy and health, *Atmos. Environ: X.*, 2025, **25**, 100308, https://doi.org/10.1016/j.aeaoa.2024.100308.

112 K. Vohra, E. A. Marais, S. Suckra, L. Kramer, W. J. Bloss, R. Sahu, A. Gaur, S. N. Tripathi, M. Van Damme, L. Clarisse and P.-F. Coheur, Long-term trends in air quality in major cities in the UK and India: a view from space, *Atmos. Chem. Phys.*, 2021, **21**, 6275–6296, https://doi.org/10.5194/acp-21-6275-2021.

113 FAO Statistics https://www.fao.org/